



Anti-inflammatory and Regulatory Effects of Huanglian Jiedu Decoction on Lipid Homeostasis and the TLR4/MyD88 Signaling Pathway in LPS-Induced Zebrafish

Junyi Zhou, Xinru Gu, Xiaorui Fan, Yanyan Zhou, Hongjie Wang, Nan Si, Jian Yang, Baolin Bian* and Haiyu Zhao*

Institute of Chinese Materia Medica, China Academy of Chinese Medical Sciences, Beijing, China

OPEN ACCESS

Edited by:

Luigi Iuliano,
Sapienza University of Rome, Italy

Reviewed by:

Yann Gilbert,
The University of Mississippi Medical
Center, United States
Francesco Peri,
University of Milano-Bicocca, Italy

*Correspondence:

Baolin Bian
blbian@icmm.ac.cn
Haiyu Zhao
hyzhao@icmm.ac.cn

Specialty section:

This article was submitted to
Lipid and Fatty Acid Research,
a section of the journal
Frontiers in Physiology

Received: 02 May 2019

Accepted: 10 September 2019

Published: 26 September 2019

Citation:

Zhou J, Gu X, Fan X, Zhou Y,
Wang H, Si N, Yang J, Bian B and
Zhao H (2019) Anti-inflammatory
and Regulatory Effects of Huanglian
Jiedu Decoction on Lipid
Homeostasis and the TLR4/MyD88
Signaling Pathway in LPS-Induced
Zebrafish. *Front. Physiol.* 10:1241.
doi: 10.3389/fphys.2019.01241

Huanglian Jiedu decoction (HLJDD) has been used in the clinical treatment of inflammatory conditions. To clarify the mechanism of its comprehensive anti-inflammatory activities, the correlation between lipid homeostasis and the TLR4/MyD88 signaling pathway in zebrafish was established in the present study. In the lipopolysaccharide (LPS)-induced inflammation in zebrafish model, RT-PCR assays of five inflammatory cytokines and six targeted proteins were measured. Lipidomics analysis was conducted to identify potential lipid markers. HLJDD displayed strong efficacies, with a 61% anti-inflammatory rate at a concentration of 50 $\mu\text{g/mL}$. The activation of TLR4/MyD88 played an essential role in the inflammatory process. All protein indexes in the HLJDD group exhibited a tendency to reverse back to normal levels. Moreover, 79 potential pathological lipid biomarkers were identified. Compared with the model group, 61 therapeutic lipid biomarkers were detected in HLJDD group. Most perturbations of lipids were ameliorated by HLJDD, mainly through the glycerophospholipid metabolic pathway. In the visual network study, the corresponding lipoproteins such as PLA₂, SGMS, and SMDP were observed as important intermediates between lipid homeostasis and the TLR4/MyD88 signaling pathway.

Keywords: Huanglian Jiedu decoction, anti-inflammatory activity, lipidomic profile, TLR4/MyD88 signaling pathway, lipopolysaccharide, zebrafish

Abbreviations: AA, arachidonic acid; APO, apolipoproteins; cDNA, complementary DNA; Cers, ceramides; cPLA₂, cytosolic PLA₂; CTL1, choline transporter like protein; dpf, days post fertilization; ERK, extracellular signal regulated kinase; FAs, fatty acids; FC, fold change; GPI, glycosylphosphatidylinositol; HLJDD, Huanglian Jiedu decoction; I κ B- α , NF- κ B inhibitor- α ; IFN- γ , interferons- γ ; IL-1 β , interleukin-1 β ; IL-10, interleukin-10; IL-6, interleukin-6; IPF, idiopathic pulmonary fibrosis; JNK, c-Jun N-terminal kinase; KEGG, Kyoto Encyclopedia of Genes and Genomes; LPS, lipopolysaccharide; LSD, least significant difference; MAPK, mitogen protein kinase; MAPK, mitogen-activated protein kinase; MTC, maximum tolerated concentration; MyD88, myeloid differentiation primary response gene 88; NF- κ B, nuclear factor- κ B; NO, nitric oxide; OPLS-DA, orthogonal projection to latent structures discriminant analysis; PA, phosphatidic acid; PCA, principal component analysis; PC-PLC, PC-specific phospholipase C; PCs, phosphatidylcholines; PEs, phosphatidylethanolamines; PGE₂, prostaglandin E₂; PKC- ζ , zeta isoform of protein kinase C; PPAR, peroxisome proliferator-activated receptor; PSs, phosphatidylserines; QC, quality control; RT-PCR, reverse transcription polymerase chain reaction; S1P, sphingosine-1 phosphate; SD, standard deviation; SMs, sphingomyelins; SphK1, sphingosine kinases 1; TGs, triglyceride; TIR, Toll/IL-1; TLR4, toll like receptors 4; TNF- α , tumor necrosis factor- α ; tR, retention time; VIP, variable importance in the projection.

INTRODUCTION

Inflammation is a complicated pathological process associated with many human diseases. It is a defense response of tissues against injury or damage (Coussens and Werb, 2002; Ryu et al., 2017). The persistence of cytokines and chemokines, as well as the triggered cascade reaction could induce tumor cell proliferation, promote inflammatory cell aggregation, and stimulate conditions such as lupus erythematosus, diabetes, cardiovascular diseases, and tumors (Wellen and Hotamisligil, 2005; Dominguez et al., 2017; Maffia and Cirino, 2017). Disorders of lipid homeostasis lead to the abnormal secretion of inflammatory mediators. Lipid oxidation and alterations in lipid structures are important triggers of inflammatory diseases, including atherosclerotic diseases, renal failure, and metabolic syndrome (Mi et al., 2012). Moreover, an exaggerated inflammatory response is able to affect intracellular lipid accumulation (Raetz et al., 2006; Colin et al., 2015). The processes of inflammation and lipid metabolism interact, and both are modulated through specific signaling pathways of NF- κ B, MAPK, and PPAR (Nakaya et al., 2011; Ayaka et al., 2015; Gong et al., 2017).

TLR4 are key membrane recognition receptors for inflammation induced by bacterial lipopolysaccharide (LPS). The TLR4 receptors are capable of activating the transcription of inflammatory molecules via stimulation of the MyD88 pathway to directly regulate the release of pro-inflammatory cytokines or the Toll/IL-1(TIR) domain-containing adaptor inducing TRIF dependent pathway to produce interferon (Thada et al., 2013; Cai et al., 2015). The MyD88 pathway, and NF- κ B and MAPK signaling pathways all comprehensively participate in the pathogenesis of inflammation and inflammatory responses. Among of them, p65, I κ B- α belong to the NF- κ B pathway. ERK, JNK, p38 belong to the MAPK pathway.

Zebrafish are highly homologous to mammals in terms of physiological signaling pathways and functions (Postlethwait et al., 2000). In recent years, zebrafish have been widely used to produce an *in vivo* model of LPS-stimulated inflammation because of their innate immune system comprising TLRs, neutrophils, and macrophages (Harvie et al., 2013; Hwang et al., 2016; Kim et al., 2018a; Ko et al., 2018). The number of neutrophils in zebrafish yolks is an important index by which the level of inflammation can be evaluated. Furthermore, the optical transparency of early developmental embryos facilitates the non-invasive and dynamic imaging of inflammation (D'Alençon et al., 2010). At present, the quantitative RT-PCR assay has become the main method of detection and examining the inflammatory factors in zebrafish models (Yang et al., 2014; Kim et al., 2018b).

HLJDD, which comprises *Coptidis Rhizoma*, *Scutellariae Radix*, *Phellodendri Chinensis Cortex*, and *Gardeniae Fructus* in the ratio 3:2:2:3, is a classical heat-clearing and detoxifying Chinese medicinal formula (Yang et al., 2013). It has been used in the treatment of inflammation-related diseases (Zhang et al., 2014; Wang et al., 2015). Furthermore, HLJDD could significantly reduce levels of inflammatory cytokines such as IL-2, TNF- α , IFN- γ , and inflammatory mediators such as prostaglandin E₂ (PGE₂) and NO to inhibit the immune

response and inflammation (Wang and Xu, 2000; Fang et al., 2004). In our previous study, qualitative and quantitative analyses of HLJDD were performed using HPLC and LC/MS methods. Berberine, baicalin, and geniposide have been identified as three major components of HLJDD (Yang et al., 2013). They reduced inflammation in a dose-dependent manner by inhibiting cytokines through NF- κ B and MAPK signaling pathways. The negative regulation of TLR4 is one important upstream mechanism of berberine, baicalin, and geniposide (Hong et al., 2012; Cui et al., 2014; Shi et al., 2014; Cheng et al., 2017; Wang et al., 2017; Zhang H. et al., 2017). In addition, the major constituents of HLJDD have also attracted increasing interest for their anti-inflammatory effects via the regulation of lipid homeostasis in fatty liver, hyperlipidemia, IPF, and other inflammation-related diseases (Gu, 2015; Hu et al., 2015; Chang et al., 2016; Meng et al., 2016; Zhang J. et al., 2017).

In the present study, HLJDD and three of its main active components exhibited significant anti-inflammatory effects in the zebrafish model of LPS-induced inflammation. Moreover, systematically non-targeted and targeted lipidomics analyses were performed to demonstrate the alterations in integrated lipid profiling after treatment with drugs. Furthermore, potential therapeutic lipid markers and their mainly metabolic pathways were identified by biofunctional analysis. Targeted proteins and cytokines regulated by the TLR4/MyD88 pathway were examined in all groups. Based on visualization and network analysis, the relationship between lipid markers and the TLR4/MyD88 signaling pathway was established via the significant intermediate bridge of corresponding lipoproteins. These findings would shed light on the clinical applications of HLJDD in inflammation-related disease.

MATERIALS AND METHODS

Chemicals and Reagents

Huanglian Jiedu decoction (a traditional Chinese herb formula) was previously prepared in our laboratory. In addition, LPS, methyl cellulose, and ammonium acetate were purchased from Sigma-Aldrich Co., (St. Louis, MO, United States). Acetonitrile, methanol, and formic acid of mass spectrometry (MS) grade were obtained from Fisher Scientific (Fair Lawn, NJ, United States). Trizol and ddH₂O (DNase/RNase Free) were purchased from Ambion (United States); HiScript Reverse Transcriptase (RNase H), 5 \times HiScript Buffer, 50 \times ROX Reference Dye 2, and SYBR Green Master Mix were purchased from VAZYME (China). Ribonuclease Inhibitor was purchased from TRANS (China); dNTP, Taq Plus DNA Polymerase, and DL2000 DNA Marker were purchased from TIANGEN (China); and Random Primer (N6) were purchased from AIDLAB (China). The standards of berberine, baicalin, and geniposide were obtained from Saibaicao Technology Co., Ltd., (Beijing, China). Indomethacin was purchased from Shanghai Jingchun Industrial Co., Ltd., (Shanghai, China). The purities of all standard references were over 98%. All other chemicals and solvents were of analytical grade.

Animal Maintenance

Zebrafish were maintained at a temperature of 28°C with a 14:10 h (day/night) cycle and fed three times per day. The quality of the rearing water was 200 mg of instant sea salt per liter of reverse osmosis water, the conductivity was 480~510 $\mu\text{S}/\text{cm}$, the hardness was 53.7~71.6 mg/L CaCO_3 , and the pH was 6.9~7.2. Transgenic zebrafish exhibiting neutrophil fluorescence (MPO-GFP) were purchased from Hunter Biotechnology, Inc., (Hangzhou, China). The MPO-GFP transgenic zebrafish line was selected for this study and all animal experiments were performed in accordance with the guidelines issued by the Animal Ethics Committee (Association for Assessment and Accreditation of Laboratory Animal Care International (AAALAC) Certificate NO.001458).

Establishment of Inflammation Model and Drug Administration

The yolks of zebrafish larva were injected with 10 mg/mL LPS at 3 days post-fertilization (dpf). A volume of 10 nL was administered to each embryo to establish the inflammatory model. Indomethacin was used as the positive control (28.6 $\mu\text{g}/\text{mL}$). Based on the maximum solubility of the substances and the tolerance of zebrafish in the maximum concentration, the MTC of HLJDD, berberine, baicalin, and geniposide in zebrafish were determined at first. The data were shown in **Supplementary Table S1**. Then in the *in vivo* susceptibility test, five concentrations of MTC/16, MTC/8, MTC/4, MTC/2, and MTC were set for each drug. Three hours after administration of the treatments, 10 transgenic zebrafish (MPO-GFP) larvae were randomly selected from each experimental group to monitor the inflammatory neutrophil migration process in real time under a fluorescence microscope. Image analysis was performed using the Nikon NIS-Elements D 3.10 advanced image processing software to calculate the number of fluorescent neutrophils (N), and quantitatively evaluate the inhibitory effect of each anti-inflammatory drug on neutrophils

in zebrafish. The formula for calculating the inhibition of inflammation was as follows:

$$\text{Extinction effect of inflammation (\%)} = \frac{[N (\text{Drug treatment group}) - N (\text{Control group})]}{N (\text{Drug treatment group})} \times 100\%$$

RNA Extraction and Quantitative Real-Time PCR

Zebrafish larvae at 3 dpf ($n = 20$) were collected for total RNA extraction, frozen in 1.5 mL micro-centrifuge tubes using liquid nitrogen, and stored at -80°C . Total RNA was isolated using the Trizol reagent (Ambion, United States), and 2 μg aliquots of total RNA were reversely transcribed into cDNA for real-time quantitative PCR using a cDNA Kit. Real-time quantitative PCR was performed with the SYBR Green Master Mix, which was used to determine the expression levels of all genes. The protocol for the real-time PCR was as follows: 50°C for 2 min; 95°C for 10 min; 40 cycles at 95°C for 30 s; followed by 60°C for 30 s. The $2^{-\Delta\Delta Ct}$ method was used to calculate the relative expression of each gene using β -actin for normalization. The experiments were repeated three times. The primer sequences used in the present study are shown in **Table 1**.

Sample Pretreatment

Zebrafish samples were thawed at room temperature. Thereafter, 1 mL of methanol/chloroform (1:3) organic solvent was added to a 1.5 mL Eppendorf tube containing each zebrafish sample. The samples were then sonicated for 10 min and vortexed for 50 min. A volume of 100 μL of water was added to each sample, following which it was centrifuged at 12 000 rpm and 4°C for 10 min. A volume of 500 μL of the supernatant was collected and snapped-frozen in liquid nitrogen, after which 200 μL of isopropanol/acetonitrile (1:1) was added for reconstitution. The samples were then sonicated and centrifuged at 12 000 rpm and 4°C for 10 min. The supernatant was then analyzed by ultra-high performance liquid chromatography coupled to Q Exactive hybrid quadrupole-Orbitrap mass spectrometry.

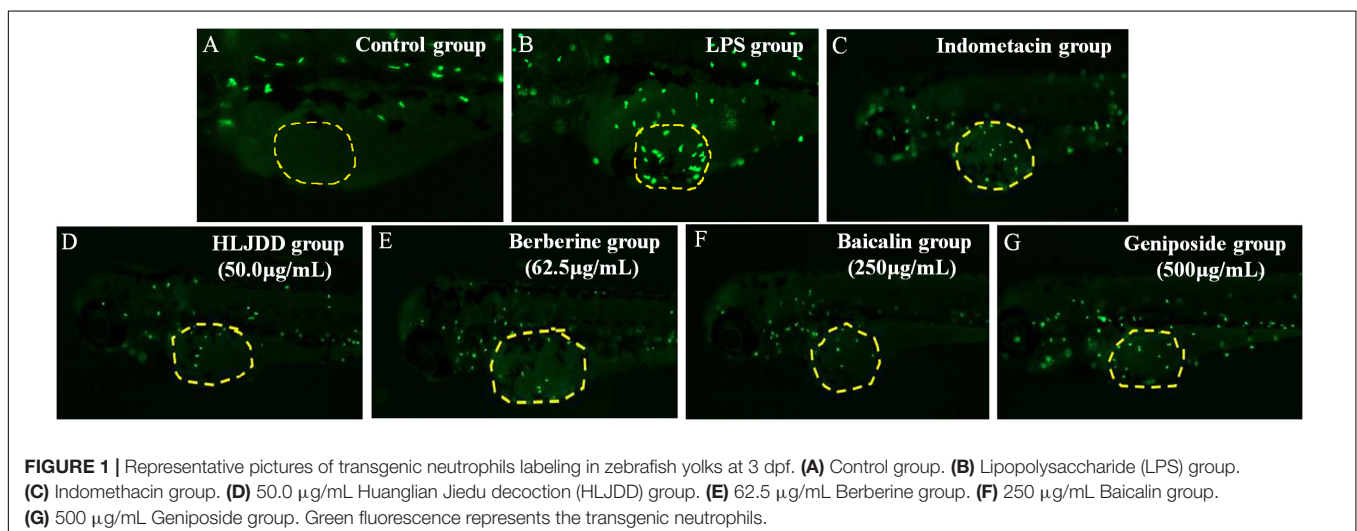


TABLE 1 | Primer sequences for the RT-PCR assay.

Gene symbol	Oligo	Primer sequence	Size (bp)
β-actin	Forward	5'- CCATCTATGAGGGTTACGC -3'	137
	Reverse	5'- GACAATTTCTCTTTTCGGCT -3'	
TNF-α	Forward	5'- GCTGGATCTTCAAAGTCGGGTGTA -3'	139
	Reverse	5'- TGTGAGTCTCAGCACACTTCCATC -3'	
IL-1β	Forward	5'- CTCAGCCTGTGTGTTGGGA -3'	209
	Reverse	5'- GGGACATTTGACGGACTCG -3'	
IL-6	Forward	5'- ACGACATCAAACACAGCACC -3'	172
	Reverse	5'- TCGATCATCAGCTGGAGAA -3'	
MyD88	Forward	5'- ACCATCGCCAGTGAGCTTAT -3'	206
	Reverse	5'- CAGATGGTCAGAAAGCGCAG -3'	
ERK	Forward	5'- TCCAAGGGCTACACCAAGTC -3'	274
	Reverse	5'- TGCGATCCAATAAATCCAAA -3'	
JNK	Forward	5'- ATTCCTTTTGTCCAGGTTT -3'	140
	Reverse	5'- TACCGTTTGAGAACCGTGAA -3'	
p38	Forward	5'- GTCGCAGAAAGAAAGACCCA -3'	130
	Reverse	5'- ATCAAACGCAGAGCAAACAG -3'	
IκB-α	Forward	5'- GTTGGATTCGTTAAAGAGGA -3'	137
	Reverse	5'- GGATAATGGCGAGATGTAGAT -3'	
p65	Forward	5'- CGCAAGAGAACTGAAGGAA -3'	205
	Reverse	5'- AGAAAAAGGAGGTGGGTGG -3'	
IL-10	Forward	5'- GGAGACCATTCTGCCAACA -3'	111
	Reverse	5'- CATTTCACCATATCCCCT -3'	
IFN-γ	Forward	5'- GTTTGCTGTTTTCGGGATGG -3'	138
	Reverse	5'- TTCGCAGGAAGATGGGGTGT -3'	

UPLC/Q-Exactive/MS Analysis

The UltiMate™ 3000 Rapid Separation LC (RSLC) system (Thermo Scientific, United States) was used for the relative quantification of different kinds of lipids. The Waters Acquity UPLC HSS T3 column (2.1 × 100 mm, 1.8 μm) was used for the separation of lipids; acetonitrile/water (60/40) was used for mobile phase A and isopropanol/acetonitrile (90/10) was used for mobile phase B. Both A and B phases contained 0.1% formic acid and 10 mmol/L ammonium acetate. The samples were eluted using the following linear gradient conditions: 0~2 min, 20~30% B; 2~5 min, 30~45% B; 5~6.5 min, 45~55% B; 6.5~12 min, 55~65% B; 12~14 min, 65~85% B; 14~17.5 min, 85~100% B; 17.5~18 min, 100~100% B, and the equilibration time was 1.5 min with 20% B. The column was operated at 45°C and the flow rate was 300 μL/min.

A Thermo Scientific™ Q Exactive hybrid quadrupole-Orbitrap mass spectrometer equipped with a HESI-II probe was employed in both positive and negative ionization modes. The HESI-II spray voltages were 3.7 kV and -3.5 kV, respectively. The heated capillary temperature was 320°C, the sheath gas pressure was 30 psi, the auxiliary gas setting was 10 psi, and the heated vaporizer temperature was 300°C. Nitrogen was used as both the sheath gas and the auxiliary gas. Nitrogen was also used as the collision gas at a pressure of 1.5 mTorr. The parameters of the full mass scan were as follows: resolution of 70,000, auto gain control target under 1.0×10^6 , maximum isolation time of 50 ms, and m/z range of 50–1500 Da.

TABLE 2 | Quantitative results of the effects among each experimental group demonstrating zebrafish inflammation (n = 10).

Group	Concentration (μg/mL)	Number of neutrophils (mean ± SE)	Anti-inflammatory effects (%)	
Control	–	2 ± 0.29	–	
LPS	–	18 ± 1.43	–	
Indomethacin	28.6	12 ± 1.00***	33***	
	HLJDD	6.25	14 ± 1.53	22
	12.5	11 ± 1.13***	39***	
	25	8 ± 0.96***	56***	
Berberine	50	7 ± 0.95***	61***	
	100	10 ± 1.58***	44***	
	3.9	16 ± 1.64	11	
	7.8	14 ± 1.00*	22*	
Baicalin	15.6	12 ± 0.73***	33***	
	31.25	9 ± 1.05***	50***	
	62.5	7 ± 0.88***	61***	
	15.6	17 ± 1.07	6	
Geniposide	31.25	13 ± 0.40***	28***	
	62.5	10 ± 0.90***	44***	
	125	9 ± 0.73***	50***	
	250	8 ± 0.54***	56***	
LPS	31.25	18 ± 1.34	0	
	62.5	15 ± 1.23	17	
	125	14 ± 0.70	22	
	250	13 ± 1.62*	28*	
500	12 ± 0.96**	33**		

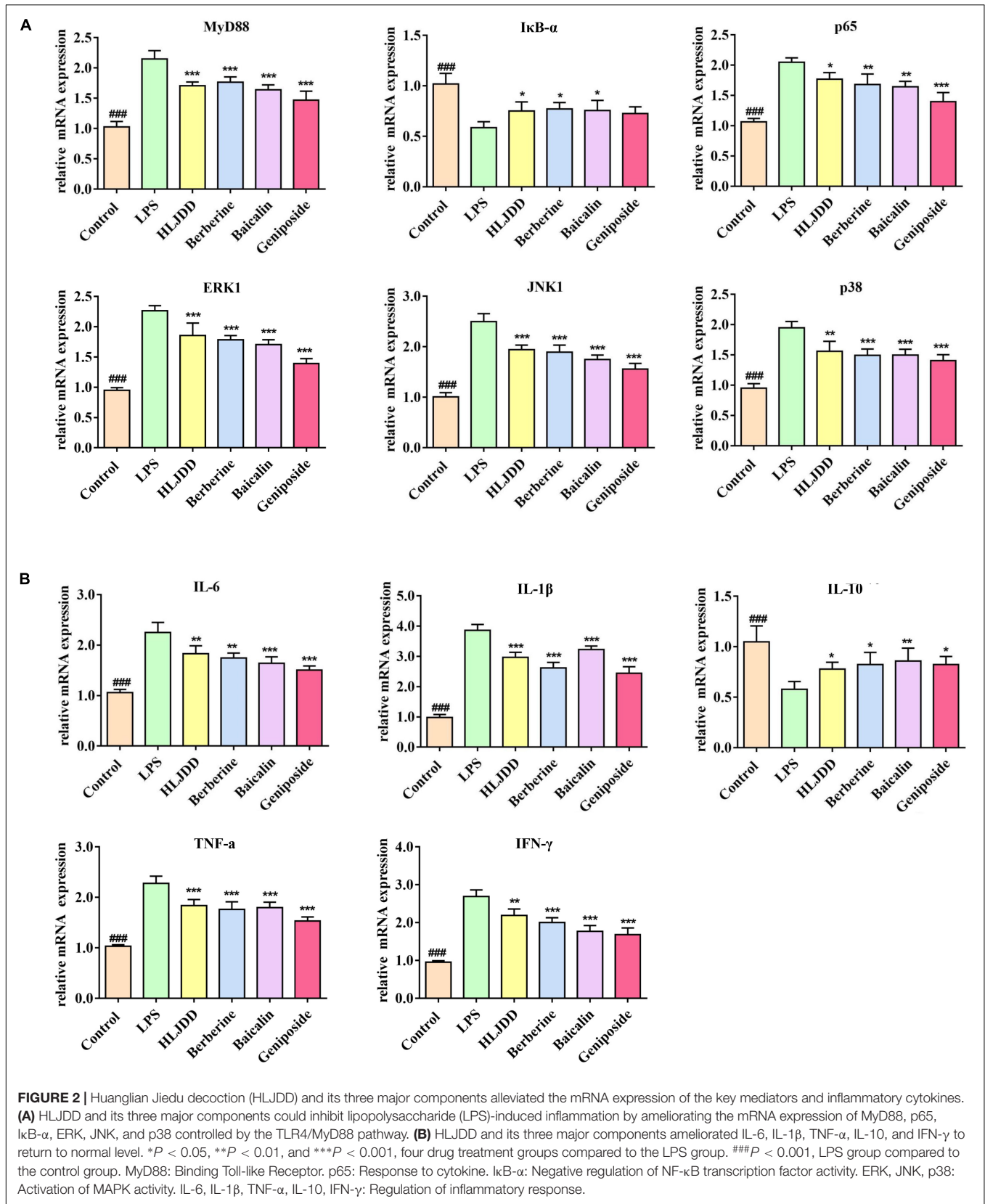
* $P < 0.05$, ** $P < 0.01$, and *** $P < 0.001$, drug treatment group (or positive group) compared with LPS group.

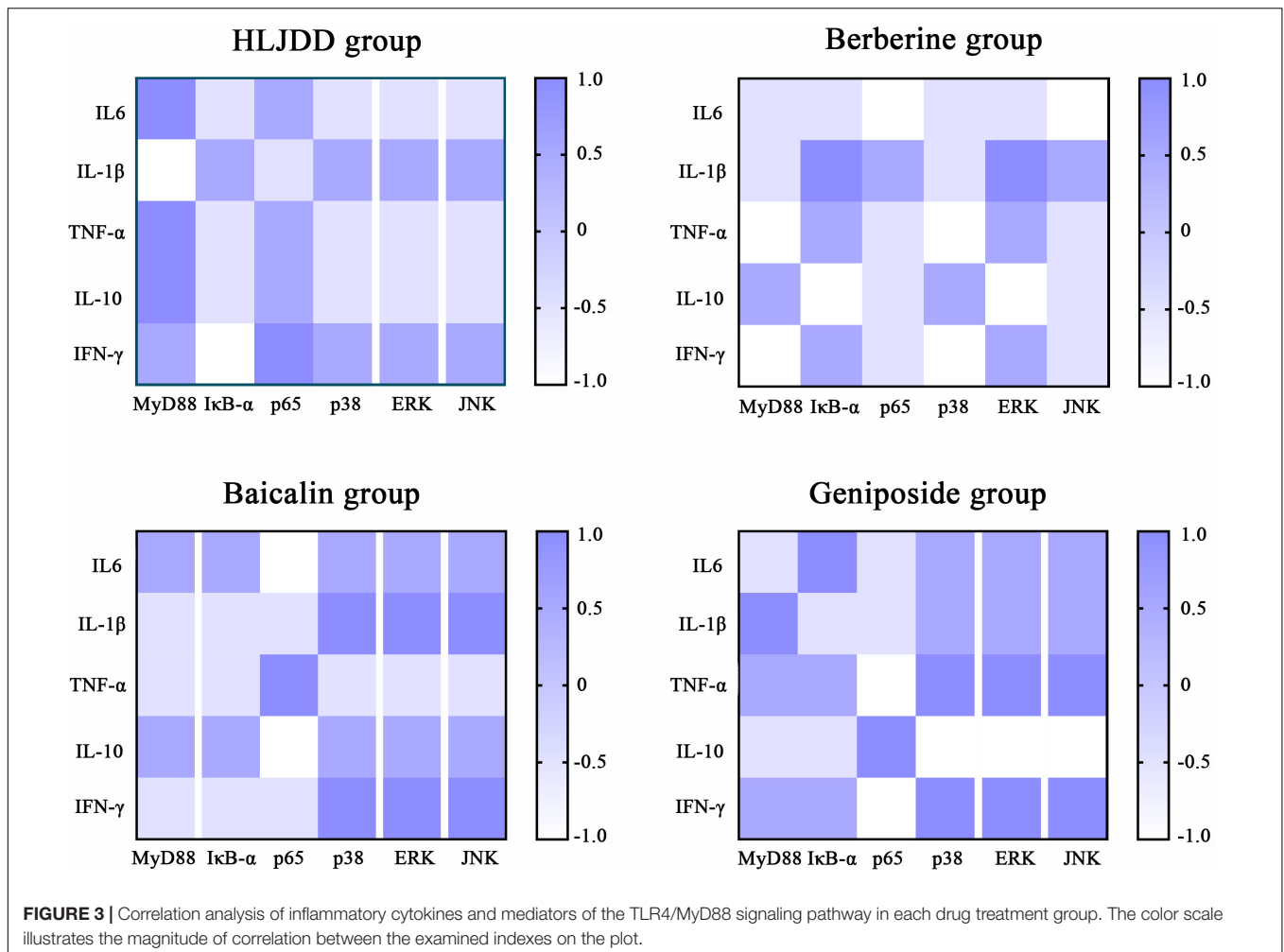
Data Processing and Statistical Analysis

All MS data in both positive and negative ion modes were processed using the Skyline software¹ for targeted lipidomics, and the Progenesis QI software (Non-linear Dynamics, Newcastle, United Kingdom) for untargeted lipidomics by imputing raw data, peak alignment, peak picking, and normalization to produce peak intensities for the retention time (t_R), m/z data pairs, and abundance. The automatic peak picking ranged from 1 to 19 min.

To monitor the stability and reproducibility of the system in each batch under analysis, QC samples were prepared by mixing equal volumes of each zebrafish sample. Three QC samples were continuously injected at the beginning of the run. Six QC samples were then injected at regular intervals throughout the analytical run in order to provide data from which repeatability could be assessed. Preprocessed data were imported to the SIMCA 14.1 software (Umetrics AB, Umea, Sweden) and EZinfo 2.0 software (Waters Corporation, Manchester, United Kingdom) for multivariate analysis. Unsupervised separation was assessed by PCA using Parteo standardization to assess the differences in the lipids of zebrafish samples among all variables. The data were further processed by OPLS-DA to identify the potential lipid markers based on

¹<http://skyline.gs.washington.edu/>





the VIP values ($VIP > 1$), t -test ($P < 0.05$), and fold change ($FC > 1.3$ or $FC < 0.7$). The external model was verified by the permutation test to evaluate the risk of overfitting. The HMDB database², and the LIPID MAPS³ and MetaboAnalyst⁴ tools were used to identify the selected potential lipid structures through multistage mass spectra information fragments and analyze the possible metabolic pathway influenced by HLJDD. R language software (x64 3.5.2) was used to install the packages (“Venn Diagram”) and (“corrplot”) for the classification and assignment of the lipid biomarkers in each group and correlation analysis. Cytoscape v3.7.1 software was used for network visualization of differentially expressed lipid marker species and the TL4R/MyD88 signaling pathway via the corresponding lipoproteins by setting the value of degree, closeness and betweenness.

All data were presented as mean \pm SD. Significant differences between the various groups were determined by one-way ANOVA, followed by LSD *post hoc* tests, using GraphPad

prism version 7.01. In all cases, a value of $P < 0.05$ was considered significant.

RESULTS AND DISCUSSION

Anti-inflammatory Effects of HLJDD, Berberine, Baicalin, and Geniposide in LPS-Stimulated Zebrafish

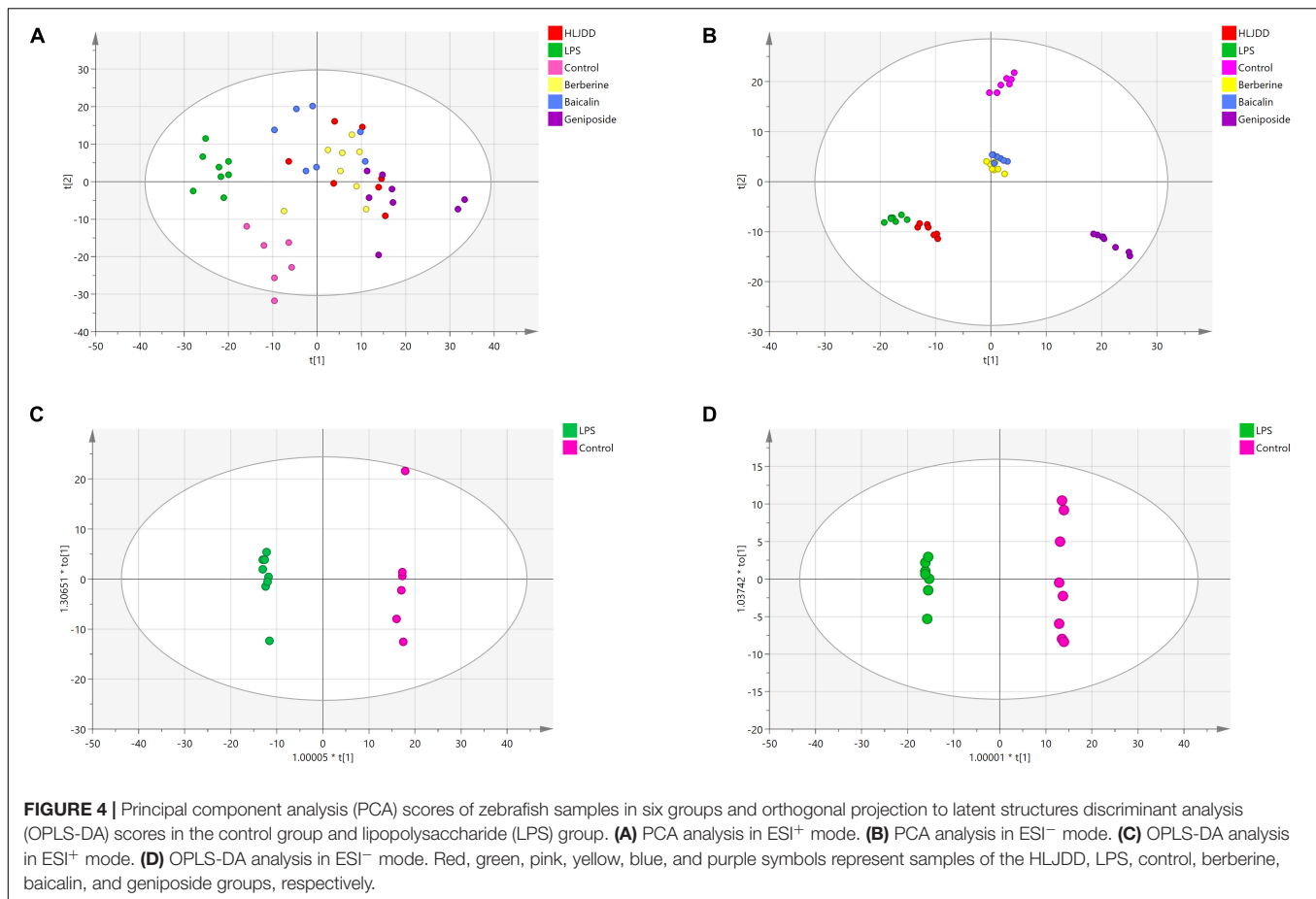
Compared with the control group, the number of neutrophils in the LPS model group was significantly increased ($P < 0.001$). The MTCs of HLJDD, berberine, baicalin, and geniposide in LPS-induced zebrafish were 100, 62.5, 250, and 500 $\mu\text{g/mL}$, respectively. Five concentrations were selected based on the MTC to evaluate the dose-effect relationships of HLJDD (6.25, 12.5, 25, 50, and 100 $\mu\text{g/mL}$); berberine (3.9, 7.8, 15.6, 31.25, and 62.5 $\mu\text{g/mL}$); baicalin (15.6, 31.25, 62.5, 125, and 250 $\mu\text{g/mL}$); and geniposide (31.25, 62.5, 125, 250, and 500 $\mu\text{g/mL}$).

The results demonstrated that HLJDD had the strongest efficacy at a concentration of 50 $\mu\text{g/mL}$ with 61% anti-inflammatory activity among four drugs. Moreover, the efficacies of berberine, baicalin, and geniposide were distinctly exhibited in

²<http://www.hmdb.ca/>

³<http://www.lipidmaps.org/>

⁴<http://www.metaboanalyst.ca/>



a concentration-dependent manner. The most favorable effects of HLJDD, berberine, baicalin, and geniposide were exhibited at concentrations of 50, 62.5, 250, and 500 $\mu\text{g}/\text{mL}$. Their anti-inflammatory activities were 61, 61, 56, and 33%, respectively. The anti-inflammatory activity of indomethacin was 33% at a concentration of 28.6 $\mu\text{g}/\text{mL}$ (Figure 1 and Table 2).

The mRNA Expression of Six Target Proteins and Five Inflammatory Cytokines

In the LPS group, the levels of $\text{I}\kappa\text{B-}\alpha$ were significantly decreased by 40%, whereas those of p65, ERK, JNK, and p38 were increased by approximately 1–2 fold greater compared with the control group. Furthermore, IL-6, IL-1 β , TNF- α , and IFN- γ were significantly induced, whereas IL-10 was reduced by the LPS stimulus. The expression of IL-1 β in the LPS group showed the greatest variation, which was approximately 4-fold greater than that in the control group. All of the aforementioned eleven indexes presented a tendency to normal levels in all of the four drug treatment groups, especially in the geniposide group. Compared with the LPS group, berberine induced a notable increase in $\text{I}\kappa\text{B-}\alpha$ levels by 30%, and IL-10 levels by 40%, and a reduction in IL-1 β levels by about 30%. Baicalin significantly increased $\text{I}\kappa\text{B-}\alpha$ levels by 30% and IL-10 levels by

50%, and simultaneously reduced JNK levels by 30% and IFN- γ levels about 30% (Figures 2A,B). Furthermore, MyD88, as the first responsive intracellular signaling molecule, played a dominant role in its association with inflammatory cytokines (O'Neill and Bowie, 2007). The phosphorylation and degradation of the $\text{I}\kappa\text{B-}\alpha$ protein led to its dissociation from NF- κB , which promoted the transfer of NF- κB into the nucleus to participate in the regulation of the expression of inflammatory cytokines (Sun and Andersson, 2002). Based on the RT-PCR results of six target proteins and five cytokines, HLJDD, berberine, baicalin, and geniposide displayed similar anti-inflammatory properties in response to LPS stimulus, which was consistent with the results of previous studies (Hong et al., 2012; Cui et al., 2014; Shi et al., 2014; Wang et al., 2017; Zhang H. et al., 2017). The results all prove that the regulation of NF- κB and MAPK signaling pathways play important roles via the anti-inflammatory mechanisms.

Based on the correlation analysis of the four drug treatment groups (Figure 3), the inflammatory cytokines and mediators of the TLR4/MyD88 pathway showed different degrees of correlation. In the HLJDD group, MyD88 was closely associated with IL-6, TNF- α , IL-1 β , and IL-10. In the baicalin group, the secretion of IL-1 β and IFN- γ via ERK, JNK, and p38 exhibited significant differences with correlation coefficients at 0.5 and 1.0, respectively. In addition, these cascade kinases and p65 were

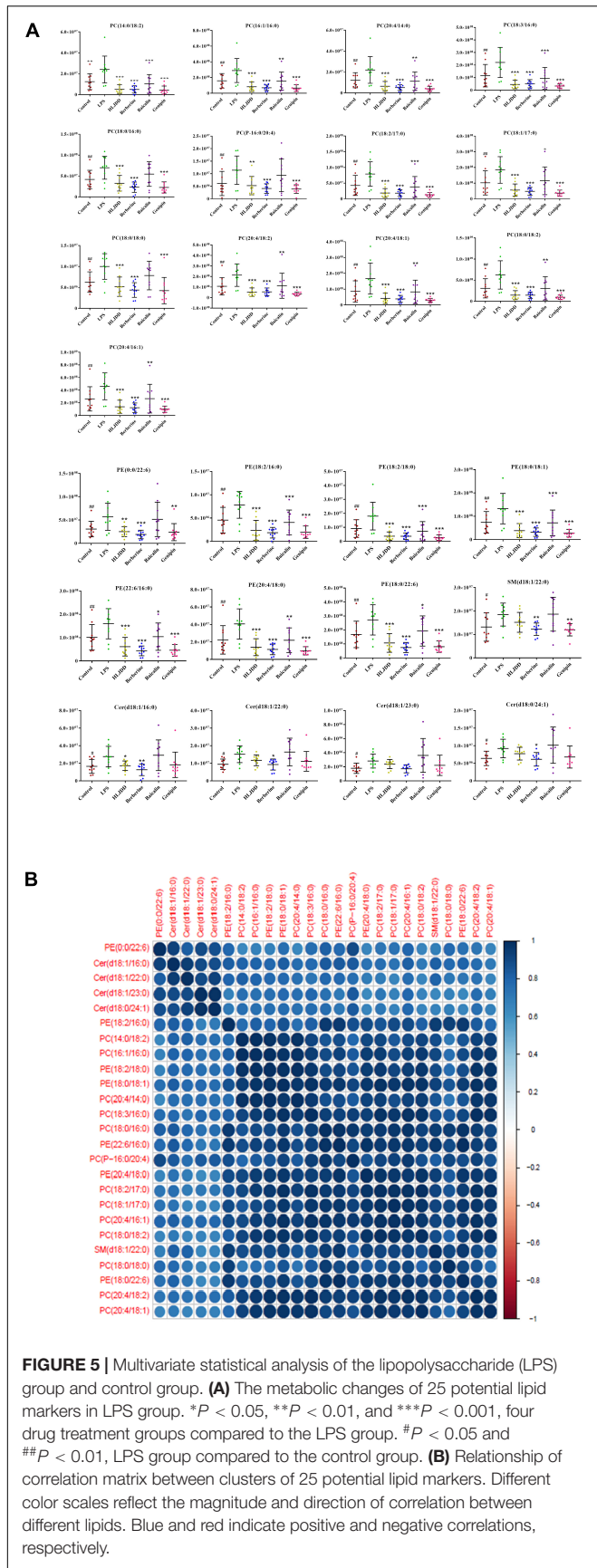


FIGURE 5 | Multivariate statistical analysis of the lipopolysaccharide (LPS) group and control group. **(A)** The metabolic changes of 25 potential lipid markers in LPS group. * $P < 0.05$, ** $P < 0.01$, and *** $P < 0.001$, four drug treatment groups compared to the LPS group. # $P < 0.05$ and ## $P < 0.01$, LPS group compared to the control group. **(B)** Relationship of correlation matrix between clusters of 25 potential lipid markers. Different color scales reflect the magnitude and direction of correlation between different lipids. Blue and red indicate positive and negative correlations, respectively.

closely associated with the secretion of TNF- α , IL-10, and IFN- γ in the geniposide group.

Identification of Non-targeted Lipid Profiling Data of Zebrafish

Based on the chromatographic retention time, accurate masses, and MS/MS fragments, 2384 positive ion peaks and 725 negative ion peaks were obtained. The plot of PCA scores exhibited distinct clusters of zebrafish in six groups. The cumulative R^2X and Q^2 were 0.824 and 0.666, respectively, in the ESI^+ mode, and 0.792 and 0.708, respectively, in the ESI^- mode (Figures 4A,B). In the plot of OPLS-DA scores, a clear separation was noted between the control group and the LPS group. The cumulative R^2Y and Q^2 were 0.998 and 0.903, respectively, in the ESI^+ mode, and 0.999 and 0.996, respectively, in the ESI^- mode (Figures 4C,D). According to the permutation test, no over-fitting tendency was evident, which indicated that the LPS-induced zebrafish inflammatory model had a favorable predictive ability for the screening of potential lipid markers. A volcano plot showed all indexes under examination. The dots indicating high ejection were considered to be very significant (Supplementary Figure S1). The levels of potential lipid markers in the LPS and drug treatment groups were screened and identified by untargeted lipidomics analysis and are presented in Supplementary Table S2. The potential lipid markers were mainly phosphatidylcholines (PCs) and phosphatidylethanolamines (PEs). The results of previous pilot experiments also support the data (Zhou et al., 2018).

Identification of Targeted Lipid Profiling Data of Zebrafish

Based on the non-targeted lipidomics results, we focused on PCs, PEs, sphingomyelins (SMs), ceramides (Cers), and triglycerides (TGs) for the analysis of targeted lipidomics. The database covered 97 PCs, 45 Cers, 27 PEs, and 24 SMs. The plot of PCA 3D scores exhibited distinct clusters of six zebrafish groups (Supplementary Figure S2).

A total of 25 pathological potential lipid markers were further discovered following induction by LPS, including 13 PCs, seven PEs, four Cers, and one SM. Specifically, PC(14:0/18:2) and PC(20:4/16:1) exhibited the highest expression in 25 biomarkers in the LPS group. After the administration of HLJDD, lipid levels of 28 PCs and eight PEs were significantly identified and exhibited a tendency to normal levels. The increase in the levels of 28 PCs and 11 PEs was reversed by the berberine treatment. In the baicalin group, 14 PCs and four PEs were identified. In the geniposide group, 33 PCs, nine PEs, and one SM were observed to have a tendency to normal levels. The identification of potential lipid markers are presented in Figure 5. The significant associations among 25 markers were assessed by correlation analysis. From a holistic view, all 25 markers were strongly correlated with each other, which supports the underlying explanation for the pathogenesis of inflammation induced by LPS. The levels of potential lipid markers in the four drug

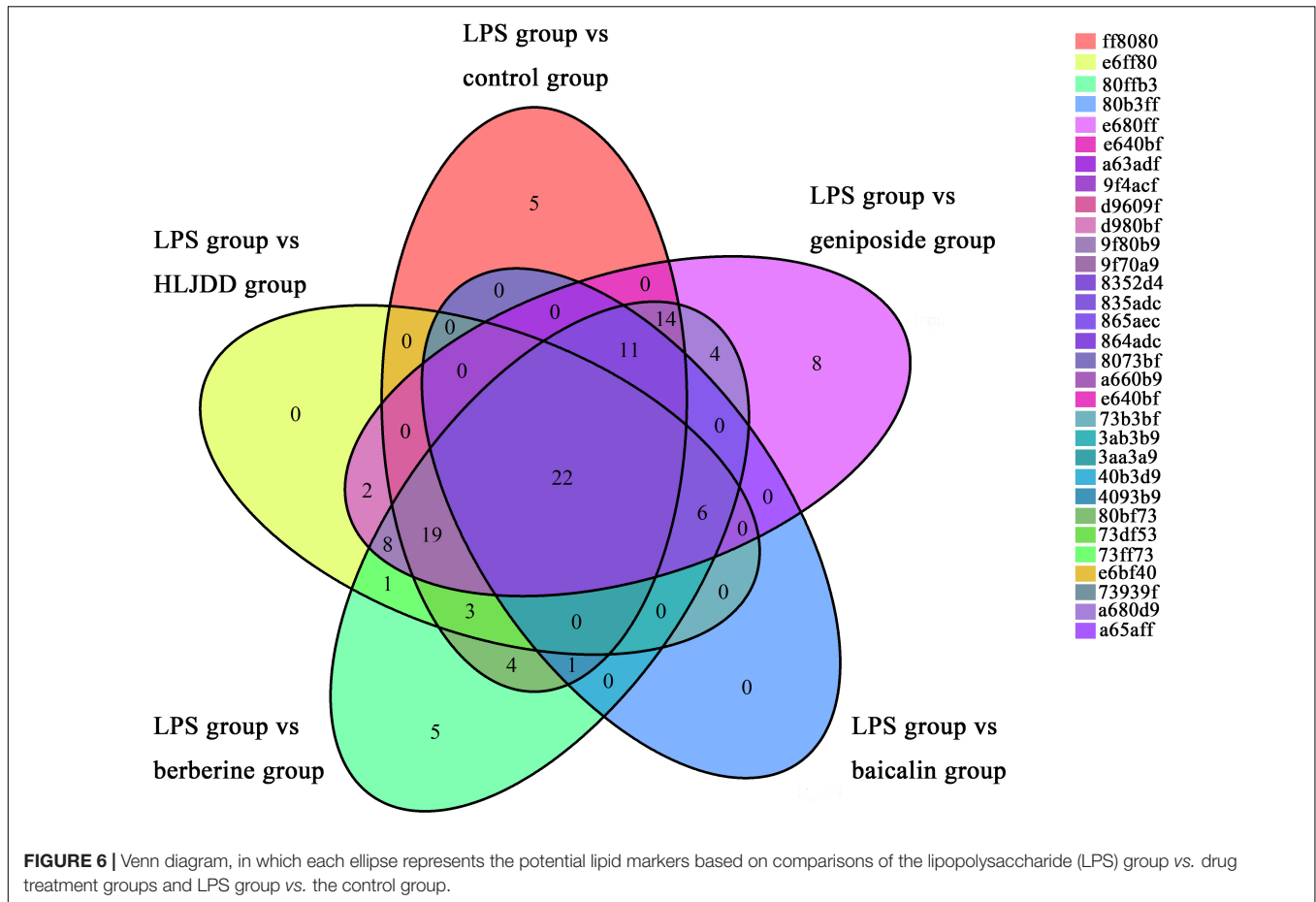


FIGURE 6 | Venn diagram, in which each ellipse represents the potential lipid markers based on comparisons of the lipopolysaccharide (LPS) group vs. drug treatment groups and LPS group vs. the control group.

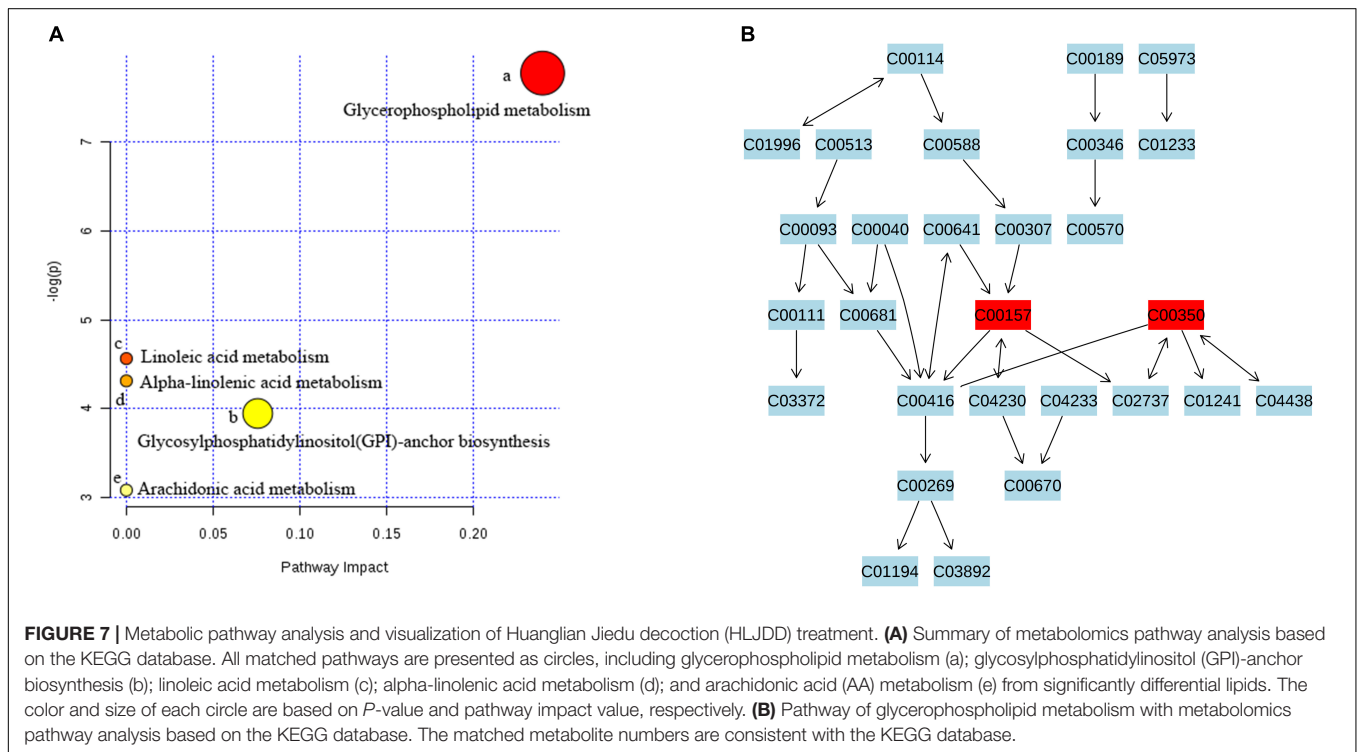
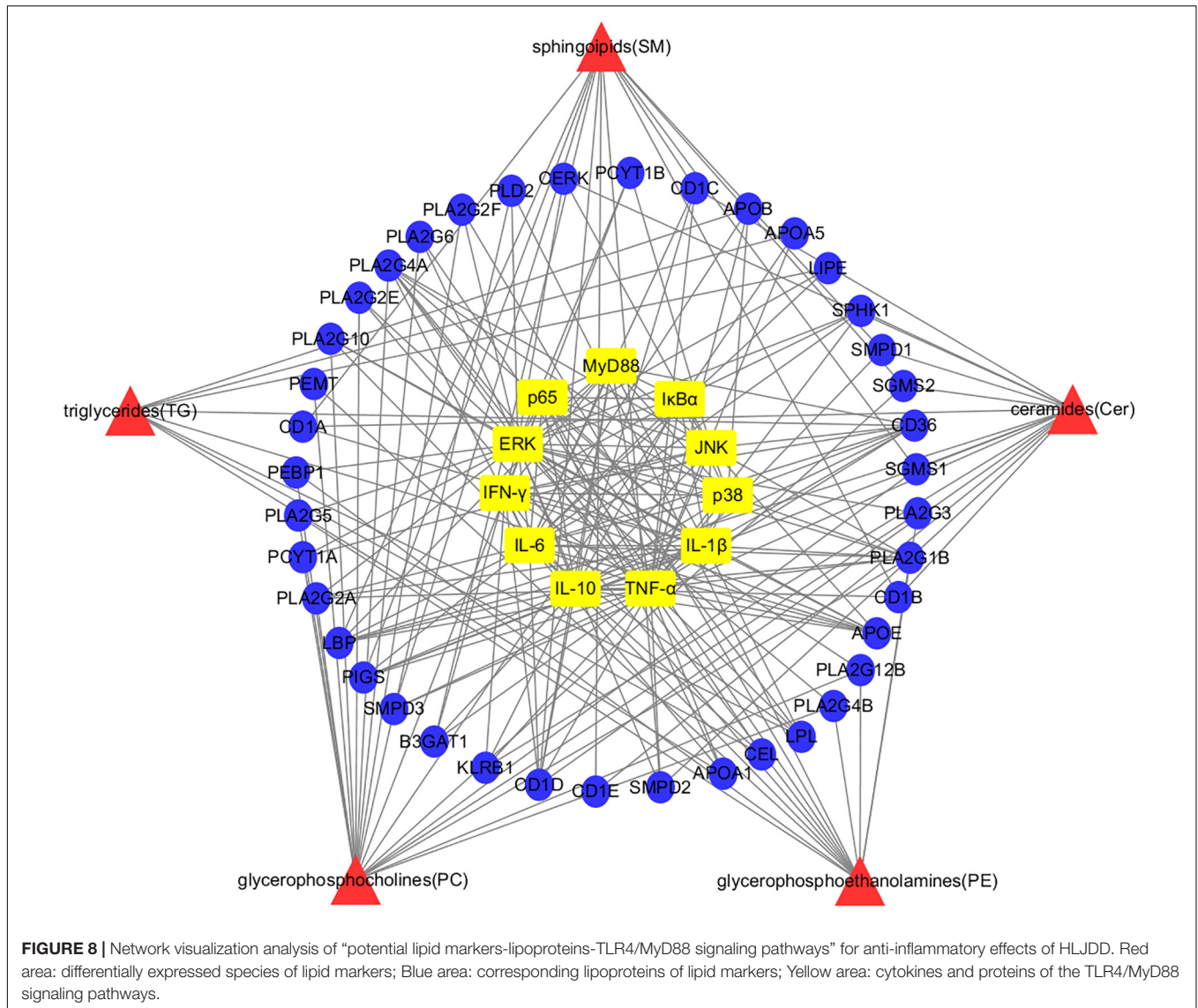


FIGURE 7 | Metabolic pathway analysis and visualization of Huanglian Jiedu decoction (HLJDD) treatment. **(A)** Summary of metabolomics pathway analysis based on the KEGG database. All matched pathways are presented as circles, including glycerophospholipid metabolism (a); glycosylphosphatidylinositol (GPI)-anchor biosynthesis (b); linoleic acid metabolism (c); alpha-linolenic acid metabolism (d); and arachidonic acid (AA) metabolism (e) from significantly differential lipids. The color and size of each circle are based on *P*-value and pathway impact value, respectively. **(B)** Pathway of glycerophospholipid metabolism with metabolomics pathway analysis based on the KEGG database. The matched metabolite numbers are consistent with the KEGG database.



treatment groups analyzed by targeted lipidomics are shown in **Supplementary Table S3**.

Metabolic Pathway Analysis of HLJDD Treatment

As shown in the Venn diagram (**Figure 6**), 22 common potential lipid markers were identified based on both targeted and non-targeted lipidomics in each group. In addition, berberine ameliorated five lipid markers, including three TGs, one PS, and one PE. Geniposide simultaneously ameliorated eight lipid markers of seven PCs and one SM. Furthermore, potential metabolic pathways influenced by HLJDD treatment were investigated for further study. Among the five important pathways under observation, glycerophospholipid metabolism was deemed the most vital metabolic pathway with the highest impact value of 0.240 (**Figure 7A**). The detailed construction of crucial metabolites in

the glycerophospholipid pathway based on the KEGG database is shown in **Figure 7B**.

Network Visualization Analysis of “Lipid Markers-Lipoproteins-TLR4/MyD88 Pathways” for the Anti-inflammatory Effects of HLJDD

Based on the HMDB database, 40 corresponding lipoproteins were retrieved according to the matching lipid markers. Correlations between differentially expressed lipid marker species and the lipoproteins associated with the TLR4/MyD88 signaling pathway was then established using network visualization analysis (**Figure 8**). The edges of the nodes in the analysis directly or indirectly interacted with each other in varying degrees. A series of PLA₂ lipoproteins were predominantly associated with PCs and PEs. Furthermore, PEMT, APO, PEBP1, and PLD2, among others were also involved in the synthesis of PCs and

PEs. The SMs and Cers interacted with SGMS, SMPD, and CD1, among others. Moreover, CD36, CEL, LPL, LIPE, and a variety of apolipoproteins (APO) were identified as the regulatory lipoproteins linking TGs to the TLR4/MyD88 signaling pathway.

The PCs and PEs accounted for a large proportion of the total number of potential lipid markers in this study. Most were polyunsaturated subclasses containing 20:4, 18:1, 18:2, and 16:1 carbon chains. After appropriate stimulation, the glycerophospholipid content, containing 16-C and 18-C fatty acid chains, was increased, which is consistent with the results of a previous study (Rouzer et al., 2007). Moreover, in the lipid metabolic network, glycerophospholipids containing a 20:4 carbon chain are important precursors of a wide range of bioactive lipid mediators, such as prostaglandins, leukotrienes, and lipoxins, among others (Mason et al., 1972; Humes et al., 1977; Scott et al., 1980; Rouzer et al., 1982; Abiko et al., 1983). The PLA₂s are limited enzymes produced by AA, PGE₂, and other bioactive substances, which play important roles in the occurrence, development, and prognosis of inflammatory diseases (Yang and Xia, 2006). cPLA₂ is produced by AA, which is from the glycerophospholipids of membranes (Murakami et al., 2011; Cao et al., 2013). In addition, owing to an up-regulation of CTLI gene transcription, LPS induced a sharp increase in PC synthesis, which affected the acute response to LPS stimulation (Snider et al., 2018). The uptake of choline was possibly restricted after administration of HLJDD, which caused the reduction in the levels of PC and alterations in cytokine secretion. The cPLA₂s were able to regulate the PKC- ζ as well, which improved the nuclear translocation of NF- κ B and enhanced the transcription of κ B-dependent vectors (Arenzana-Seisdedos et al., 1993). Moreover, the dependence of PC-PLC on LPS-mediated activation of PKC- ζ is also associated with the activation of MAPK ERK 1/2 (Monick et al., 1999), which is a downstream signal of PKC (Lin and Zhang, 1996).

The levels of SMs and Cers were regulated by SGMS and SMPD in the SM cycle. Overexpression of SGMS₁ and SGMS₂ enhanced apoptosis mediated by the activation of DAG and PKC. As a neutral hydrolase, SMPD₃ inhibited both proliferation and the cell cycle via SM hydrolysis, as well as the succeeding increase in the levels of Cers. The lack of SGMS₂ resulted in the degradation of NF- κ B and the expression of related genes (Hailemariam et al., 2008; Libby, 2012). The CD₁ family comprises crucial structures that are required for interactions between accessory cells and T cells. Furthermore, SM is bound to the CD1D isoform. The CD-I type participates in the regulation of inflammation (Cox et al., 2009).

The main source of Cers is SMs, which are involved in a variety of important cellular signaling pathways and physiological processes (Hannun and Obeid, 2008). The Cers are considered important second signal effector molecules (Cuschieri, 2006). They activate the NF- κ B and MAPK/JNK cascade signaling pathways, and up-regulate transcription factors associated with inflammation (Brenner et al., 1997; Shirakabe et al., 1997; Bourbon et al., 2000). The Cers are also hydrolyzed to sphingosine and then phosphorylated to S1P by SphK1 (Maceyka and Spiegel, 2014). All of these enzymes

could regulate the activation of TLR4 stimulated by LPS (Vallabhapurapu and Karin, 2009).

The metabolism of TGs has a strong correlation with inflammation. The transport of TGs in lipoproteins is facilitated by polar lipids comprising phospholipids, a variety of APOs and unesterified cholesterol (Welty, 2013). As a co-receptor for TLRs in the recognition of pathogen-associated lipids, CD36 contributes to inflammatory resolution (Stuart et al., 2005; Ballesteros et al., 2014). One of its physiological functions is the high-affinity uptake of long-chain FAs from TG-rich lipoproteins. Furthermore, CD36 affects the remodeling of myocardial phospholipids and eicosanoid production. In cases of excessive FA supply, CD36 leads to lipid accumulation, dysfunction, and inflammation (Abumrad and Goldberg, 2016).

CONCLUSION

In the present study, a total of 79 aberrantly changed lipid markers were confirmed in the LPS model group. Furthermore, 61 lipid markers were differentially expressed in the HLJDD treatment group, most of which were associated with PCs, PEs, SMs, Cers, and TGs. HLJDD played an important role in attenuating LPS-induced inflammation.

The visualization network correlation analysis of lipid biomarkers and the TLR4/MyD88 signaling pathways demonstrated that lipid homeostasis is a significant anti-inflammatory mechanism of HLJDD. In addition, lipoproteins were found to be a significant intermediate bridge between lipid metabolism and inflammatory pathways. Further research should be conducted to validate the role of lipoproteins and their association with the anti-inflammatory effects of HLJDD.

DATA AVAILABILITY STATEMENT

All datasets generated for this study are included in the manuscript/**Supplementary Files**.

AUTHOR CONTRIBUTIONS

JZ wrote the manuscript and performed the experiments. XG, XF, and YZ performed the experiments. HW, NS, and JY analyzed the data. BB and HZ designed the experiments. All authors reviewed the final manuscript.

FUNDING

This research was supported by grants from the National Natural Science Foundation of China (No. 81202904).

SUPPLEMENTARY MATERIAL

The Supplementary Material for this article can be found online at: <https://www.frontiersin.org/articles/10.3389/fphys.2019.01241/full#supplementary-material>

REFERENCES

- Abiko, Y., Shibata, Y., Fukushima, K., Murai, S., and Takiguchi, H. (1983). The stimulation of macrophage prostaglandin E2 and thromboxane B2 secretion by *Streptococcus mutans* insoluble glucans. *FEBS Lett.* 154, 297–300. doi: 10.1016/0014-5793(83)80170-7
- Abumrad, N. A., and Goldberg, I. J. (2016). CD36 actions in the heart: lipids, calcium, inflammation, repair and more? *Biochim. Biophys. Acta* 1861, 1442–1449. doi: 10.1016/j.bbali.2016.03.015
- Arenzana-Seisdedos, F., Fernandez, B., Dominguez, I., Jacqué, J. M., Thomas, D., Diaz-Meco, M. T., et al. (1993). Phosphatidylcholine hydrolysis activates NF-kappa B and increases human immunodeficiency virus replication in human monocytes and T lymphocytes. *J. Virol.* 67, 6596–6604. doi: 10.1016/0166-0934(93)90145-H
- Ayaka, I., Cynthia, H., Xin, R., Zhu, X., Tarling, E. J., Hedde, P. N., et al. (2015). LXRs link metabolism to inflammation through abca1-dependent regulation of membrane composition and TLR signaling. *eLife* 4:e08009. doi: 10.7554/eLife.08009
- Ballesteros, I., Cuartero, M. I., Pradillo, J. M., de la Parra, J., Perez-Ruiz, A., Corbi, A., et al. (2014). Rosiglitazone-induced CD36 up-regulation resolves inflammation by PPARgamma and 5-LO-dependent pathways. *J. Leukoc. Biol.* 95, 587–598. doi: 10.1189/jlb.0613326
- Bourbon, N. A., Yun, J., and Kester, M. (2000). Ceramide directly activates protein kinase C ζ to regulate a stress-activated protein kinase signaling complex. *J. Biol. Chem.* 275, 35617–35623. doi: 10.1074/jbc.M007346200
- Brenner, B., Koppenhoefer, U., Weinstock, C., Linderkamp, O., Lang, F., and Gulbins, E. (1997). Fas-or ceramide-induced apoptosis is mediated by a Rac1-regulated activation of Jun N-terminal kinase/p38 kinases and GADD153. *J. Biol. Chem.* 272, 22173–22181. doi: 10.1074/jbc.272.35.22173
- Cai, B. G., Zhu, J., and Wang, M. R. (2015). Progress of toll-like receptor 4 signaling pathway. *J. Med. Postgra.* 28, 1228–1232. doi: 10.16571/j.cnki.1008-8199.2015.11.026
- Cao, J., Burke, J. E., and Dennis, E. A. (2013). Using hydrogen/deuterium exchange mass spectrometry to define the specific interactions of the phospholipase A2 superfamily with lipid substrates, inhibitors, and membranes. *J. Biol. Chem.* 288, 1806–1813. doi: 10.1074/jbc.R112.421909
- Chang, X., Wang, Z., Zhang, J., Yan, H., Bian, H., Xia, M., et al. (2016). Lipid profiling of the therapeutic effects of berberine in patients with nonalcoholic fatty liver disease. *J. Transl. Med.* 14:266. doi: 10.1186/s12967-016-0982-x
- Cheng, P., Wang, T., Li, W., Muhammad, I., Wang, H., Sun, X., et al. (2017). Baicalin alleviates lipopolysaccharide-induced liver inflammation in chicken by suppressing TLR4-mediated NF-kB pathway. *Front. Pharmacol.* 8:547. doi: 10.3389/fphar.2017.00547
- Colin, S., Chinetti, G. G., and Staels, B. (2015). Macrophage phenotypes in atherosclerosis. *Immunol. Rev.* 262, 153–166. doi: 10.1111/immr.12218
- Coussens, L. M., and Werb, Z. (2002). Inflammation and cancer. *Nature* 420, 860–867. doi: 10.1007/978-3-0348-0837-8
- Cox, D., Fox, L., Tian, R., Bardet, W., Skaley, M., Mojsilovic, D., et al. (2009). Determination of cellular lipids bound to human cd1d molecules. *PLoS One* 4:e5325. doi: 10.1371/journal.pone.0005325
- Cui, L., Feng, L., Zhang, Z. H., and Jia, X. B. (2014). The anti-inflammation effect of baicalin on experimental colitis through inhibiting TLR4/NF-kB pathway activation. *Int. Immunopharmacol.* 23, 294–303. doi: 10.1016/j.intimp.2014.09.005
- Cuschieri, J. (2006). Phosphatidylcholine-specific phospholipase C (PC-PLC) is required for LPS-mediated macrophage activation through CD14. *J. Leukoc. Biol.* 80, 407–414. doi: 10.1189/jlb.1105622
- D'Alençon, C. A., Peña, O. A., Wittmann, C., Gallardo, V. E., Jones, R. A., Loosli, F., et al. (2010). A high-throughput chemically induced inflammation assay in zebrafish. *BMC Biol.* 8:151. doi: 10.1186/1741-7007-8-151
- Dominguez, C., David, J. M., and Palena, C. (2017). Epithelial-mesenchymal transition and inflammation at the site of the primary tumor. *Semin. Cancer Biol.* 47, 177–184. doi: 10.1016/j.semcancer.2017.08.002
- Fang, Q., Zhan, X. P., Mo, J. L., and Sun, M. (2004). Therapeutic effect of huanglian jiedu decoction on AD rats and its effect on cytokine content. *Chin. J. Chin. Mater. Med.* 29, 575–578.
- Gong, Y. Z., Sun, S. W., and Liao, D. F. (2017). Interaction and regulation of cell inflammation and lipid metabolism. *Chin. J. Arterioscler.* 25, 623–629. doi: 10.3969/j.issn.1007-3949.2017.06.016
- Gu, S. H. (2015). Metabolomic and pharmacokinetic study on the mechanism underlying the lipid-lowering effect of oral-administrated berberine. *Mol. Biosyst.* 11, 463–474. doi: 10.1039/c4mb90042a
- Hailemariam, T. K., Huan, C., Liu, J., Li, Z., Roman, C., Kalbfleisch, M., et al. (2008). Sphingomyelin synthase 2 deficiency attenuates NF-kB activation. *Arterioscler. Thromb. Vasc. Biol.* 28, 1519–1526. doi: 10.1161/ATVBAHA.108.168682
- Hannun, Y. A., and Obeid, L. M. (2008). Principles of bioactive lipid signalling: lessons from sphingolipids. *Nat. Rev. Mol. Cell Biol.* 9, 139–150. doi: 10.1038/nrm2329
- Harvie, E. A., Green, J. M., Neely, M. N., and Huttenlocher, A. (2013). Innate immune response to *Streptococcus iniae* infection in zebrafish larvae. *Infect. Immun.* 81, 110–121. doi: 10.1128/IAI.00642-12
- Hong, T., Yang, Z., Lv, C. F., and Zhang, Y. (2012). Suppressive effect of berberine on experimental dextran sulfate sodium-induced colitis. *Immunopharmacol. Immunotoxicol.* 34, 391–397. doi: 10.3109/08923973.2011.609887
- Hu, C., Wang, Y., Fan, Y., Li, H., Wang, C., Zhang, J., et al. (2015). Lipidomics revealed idiopathic pulmonary fibrosis-induced hepatic lipid disorders corrected with treatment of baicalin in a murine model. *AAPS J.* 17, 711–722. doi: 10.1208/s12248-014-9714-4
- Humes, J. L., Bonney, R. J., Pelus, L., Dahlgren, M. E., Sadowski, S. J., Kuehl, F. A. Jr., et al. (1977). Macrophages synthesis and release prostaglandins in response to inflammatory stimuli. *Nature* 269, 149–151. doi: 10.1038/269149a0
- Hwang, J. H., Kim, K. J., Ryu, S. J., and Lee, B. Y. (2016). Caffeine prevents LPS-induced inflammatory responses in RAW264.7 cells and zebrafish. *Chem. Biol. Interact.* 248, 1–7. doi: 10.1016/j.cbi.2016.01.020
- Kim, E. A., Ding, Y., Yang, H. W., Heo, S. J., and Lee, S. H. (2018a). Soft coral *Dendronephthya puetteri* extract ameliorates inflammations by suppressing inflammatory mediators and oxidative stress in LPS-stimulated zebrafish. *Int. J. Mol. Sci.* 19:2695. doi: 10.3390/ijms19092695
- Kim, E. A., Kim, S. Y., Ye, B. R., Kim, J., Ko, S. C., Lee, W. W., et al. (2018b). Anti-inflammatory effect of Apo-9'-fucoxanthinone via inhibition of MAPKs and NF-kB signaling pathway in LPS-stimulated RAW 264.7 macrophages and zebrafish model. *Int. Immunol.* 59, 339–346. doi: 10.1016/j.intimp.2018.03.034
- Ko, E. Y., Heo, S. J., Cho, S. H., Lee, W., Kim, S. Y., Yang, H. W., et al. (2018). 3-Bromo-5-(ethoxymethyl)-1,2-benzenediol inhibits LPS-induced pro-inflammatory responses by preventing ROS production and downregulating NF-kB in vitro and in a zebrafish model. *Int. Immunol.* 8, 98–105. doi: 10.1016/j.intimp.2018.11.021
- Libby, P. (2012). Inflammation in atherosclerosis. *Arterioscler. Thromb. Vasc. Biol.* 32, 2045–2051. doi: 10.1161/ATVBAHA.108.179705
- Lin, M. Q., and Zhang, Z. L. (1996). Activation and translocation of protein kinase C and its signaling pathway. *Life Sci.* 1, 15–18.
- Maceyka, M., and Spiegel, S. (2014). Sphingolipid metabolites in inflammatory disease. *Nature* 510, 58–67. doi: 10.1038/nature13475
- Maffia, P., and Cirino, G. (2017). Targeting inflammation to reduce cardiovascular disease risk. *Br. J. Pharmacol.* 174, 3895–3897. doi: 10.1111/bph.14039
- Mason, R. J., Stosel, T. P., and Vaughan, M. (1972). Lipids of alveolar macrophages, polymorphonuclear leukocytes, and their phagocytic vesicles. *J. Clin. Invest.* 51, 2399–2407. doi: 10.1172/JCI107052
- Meng, S. X., Liu, Q., Tang, Y. J., Wang, W. J., Zheng, Q. S., Tian, H. J., et al. (2016). A Recipe composed of chinese herbal active components regulates hepatic lipid metabolism of NAFLD in vivo and in vitro. *Biomed. Res. Int.* 2016, 1–12. doi: 10.1155/2016/1026852
- Mi, N., Ji, Z. X., and Wu, C. E. (2012). Effect of lipid on inflammation. *Int. J. Pathol. Clin.* 32, 421–426. doi: 10.3969/j.issn.1672-7347.2012.05.011
- Monick, M. M., Carter, A. B., Gudmundsson, G., Mallampalli, R., Powers, L. S., and Hunninghake, G. W. (1999). A phosphatidylcholine-specific phospholipase C regulates activation of p42/44 mitogen-activated protein kinases in lipopolysaccharide-stimulated human alveolar macrophages. *J. Immunol.* 162, 3005–3012.
- Murakami, M., Taketomi, Y., Miki, Y., Sato, H., Hirabayashi, T., and Yamamoto, K. (2011). Recent progress in phospholipase A2 research: from cells to animals to humans. *Prog. Lipid Res.* 50, 152–192. doi: 10.1016/j.plipres.2010.12.001
- Nakaya, K., Tohyama, J., Naik, S. U., Tanigawa, H., MacPhee, C., Billheimer, J. T., et al. (2011). Peroxisome proliferator-activated receptor- α activation

- promotes macrophage reverse cholesterol transport through a liver X receptor-dependent pathway. *Arterioscler. Thromb. Vasc. Biol.* 31, 1276–1282. doi: 10.1161/ATVBAHA.111.225383
- O'Neill, L. A., and Bowie, A. G. (2007). The family of five: TIR-domain-containing adaptors in Toll-like receptor signalling. *Nat. Rev. Immunol.* 7, 353–364. doi: 10.1038/nri2079
- Postlethwait, J. H., Woods, I. G., Ngo-Hazelett, P., Yan, Y. L., Kelly, P. D., Chu, F., et al. (2000). Zebrafish comparative genomics and the origins of vertebrate chromosomes. *Genome Res.* 10, 1890–1902. doi: 10.1101/gr.164800
- Raetz, C. R., Garrett, T. A., Reynolds, C. M., Shaw, W. A., Moore, J. D., Smith, D. C. Jr., et al. (2006). Kdo2-lipid A of *Escherichia coli*, a defined endotoxin that activates macrophages via TLR-4. *J. Lipid Res.* 47, 1097–1111. doi: 10.1194/jlr.M600027-JLR200
- Rouzer, C. A., Ivanova, P. T., Byrne, M. O., Brown, H. A., and Marnett, L. J. (2007). Lipid profiling reveals glycerophospholipid remodeling in zymosan-stimulated macrophages. *Biochemistry* 46, 6026–6042. doi: 10.1021/bi0621617
- Rouzer, C. A., Scott, W. A., Hamill, A. L., Liu, F. T., Katz, D. H., and Cohn, Z. A. (1982). IgE immune complexes stimulate arachidonic acid release by mouse peritoneal macrophages. *Proc. Natl. Acad. Sci. U.S.A.* 79, 5656–5660. doi: 10.1073/pnas.79.18.5656
- Ryu, H. W., Lee, S. U., Lee, S., Song, H. H., Son, T. H., Kim, Y. U., et al. (2017). 3-Methoxy-catalposide inhibits inflammatory effects in lipopolysaccharide-stimulated RAW264.7 macrophages. *Cytokine* 91, 57–64. doi: 10.1016/j.cyt.2016.12.006
- Scott, W. A., Zrike, J. M., Hamill, A. L., Kempe, J., and Cohn, Z. A. (1980). Regulation of arachidonic acid metabolites in macrophages. *J. Exp. Med.* 152, 324–335. doi: 10.1084/jem.152.2.324
- Shi, Q. H., Cao, J. J., Zhao, H. Y., Zhao, H., Liu, Z., Ran, J., et al. (2014). Geniposide suppresses LPS-induced nitric oxide, PGE2 and inflammatory cytokine by downregulating NF- κ B, MAPK and AP-1 signaling pathways in macrophages. *Int. Immunol.* 20, 298–306. doi: 10.1016/j.intimp.2014.04.004
- Shirakabe, K., Yamaguchi, K., Shibuya, H., Irie, K., Matsuda, S., Moriguchi, T., et al. (1997). TAK1 mediates the ceramide signaling to stress-activated protein kinase/c-Jun N-terminal kinase. *J. Biol. Chem.* 272, 8141–8144. doi: 10.1074/jbc.272.13.8141
- Snider, S. A., Margison, K. D., Ghorbani, P., LeBlond, N. D., O'Dwyer, C., Nunes, J. R. C., et al. (2018). Choline transport links macrophage phospholipid metabolism and inflammation. *J. Biol. Chem.* 293, 11600–11611. doi: 10.1074/jbc.RA118.003180
- Stuart, L. M., Deng, J., Silver, J. M., Takahashi, K., Tseng, A. A., Hennessy, E. J., et al. (2005). Response to *Staphylococcus aureus* requires CD36-mediated phagocytosis triggered by the COOH-terminal cytoplasmic domain. *J. Cell Biol.* 170, 477–485. doi: 10.1083/jcb.200501113
- Sun, Z. W., and Andersson, R. (2002). NF-kappa B activation and inhibition: a review. *Shock* 18, 99–106. doi: 10.1097/00024382-200208000-00001
- Thada, S., Valluri, V. L., and Gaddam, S. L. (2013). Influence of toll-like receptor gene polymorphisms to tuberculosis susceptibility in humans. *Scand. J. Immunol.* 78, 221–229. doi: 10.1111/sji.12066
- Vallabhapurapu, S., and Karin, M. (2009). Regulation and function of NF-kappa B transcription factors in the immune system. *Annu. Rev. Immunol.* 27, 693–733. doi: 10.1146/annurev.immunol.021908.132641
- Wang, J., Chen, L., Liang, Z., Li, Y., Yuan, F., Liu, J., et al. (2017). Genipin inhibits LPS-induced inflammatory response in BV2 microglial cells. *Neurochem. Res.* 42, 1–8. doi: 10.1007/s11064-017-2289-6
- Wang, L. J., and Xu, Q. (2000). Study on anti-inflammatory mechanism of huanglian jiedu decoction. *Chin. J. Chin. Mater. Med.* 20, 493–495. doi: 10.3321/j.issn:1001-5302.2000.08.017
- Wang, R. L., Li, X. J., Bai, Y. F., Wang, L. F., Li, B., Li, Y. G., et al. (2015). Preventive effects of huanglian jiedu decoction on alcoholic fatty liver in mice. *Chin. J. Comp. Med.* 25, 34–37.
- Wellen, K. E., and Hotamisligil, G. S. (2005). Inflammation, stress, and diabetes. *J. Clin. Invest.* 115, 1111–1119. doi: 10.1172/JCI200525102
- Welty, F. K. (2013). How do elevated triglycerides and low HDL-cholesterol affect inflammation and atherothrombosis? *Curr. Cardiol. Rep.* 15:400. doi: 10.1007/s11886-013-0400-4
- Yang, L. L., Wang, G. Q., Yang, L. M., Huang, Z. B., Zhang, W. Q., and Yu, L. Z. (2014). Endotoxin molecule lipopolysaccharide-induced zebrafish inflammation model: a novel screening method for anti-inflammatory drugs. *Molecules* 19, 2390–2409. doi: 10.3390/molecules19022390
- Yang, Y., Wang, H. J., Yang, J., Brantner, A. H., Lower-Nedza, A. D., Si, N., et al. (2013). Chemical profiling and quantification of Chinese medicinal formula huang-lian-jie-du decoction, a systematic quality control strategy using ultra high performance liquid chromatography combined with hybrid quadrupole-orbitrap and triple quadrupole mass spectrometers. *J. Chromatogr. A* 1321, 88–99. doi: 10.1016/j.chroma.2013.10.072
- Yang, Y. Z., and Xia, S. H. (2006). The role of phospholipase A 2 in inflammatory responses. *WCJD* 14, 795–799. doi: 10.3969/j.issn.1009-3079.2006.08.011
- Zhang, H., Shan, Y., Wu, Y., Xu, C., Yu, X., Zhao, J., et al. (2017). Berberine suppresses LPS-induced inflammation through modulating Sirt1/NF- κ B signaling pathway in RAW264.7 cells. *Int. Immunol.* 52, 93–100. doi: 10.1016/j.intimp.2017.08.032
- Zhang, J., Zhang, H., Deng, X., Zhang, N., Liu, B., Xin, S., et al. (2017). Baicalin attenuates non-alcoholic steatohepatitis by suppressing key regulators of lipid metabolism, inflammation and fibrosis in mice. *Life Sci.* 192, 46–54. doi: 10.1016/j.lfs.2017.11.027
- Zhang, X., He, Q., Lei, F. F., Li, R. G., and Tan, H. B. (2014). Research progress of huanglian jiedu decoction in the treatment of metabolic diseases based on inflammation theory. *Int. J. Trad. Chin. Med.* 36, 84–86. doi: 10.3760/cma.j.issn.1673-4246.2014.01.028
- Zhou, J. Y., Zhou, Y. Y., Bian, B. L., Wang, H. J., Si, N., Yang, J., et al. (2018). LPS-stimulated zebrafish inflammatory excess-heat model and lipid biomarkers screening. *J. Zhejiang Chin. Med. Univ.* 42, 782–789. doi: 10.16466/j.issn1005-5509.2018.10.003

Conflict of Interest: The authors declare that the research was conducted in the absence of any commercial or financial relationships that could be construed as a potential conflict of interest.

Copyright © 2019 Zhou, Gu, Fan, Zhou, Wang, Si, Yang, Bian and Zhao. This is an open-access article distributed under the terms of the Creative Commons Attribution License (CC BY). The use, distribution or reproduction in other forums is permitted, provided the original author(s) and the copyright owner(s) are credited and that the original publication in this journal is cited, in accordance with accepted academic practice. No use, distribution or reproduction is permitted which does not comply with these terms.